

Random quasi-phase-matched nonlinear optical conversion of supercontinuum to the ultraviolet

A. S. Aleksandrovsky,^{1,2,a)} A. M. Vyunishev,^{1,2} A. I. Zaitsev,^{1,2} and V. V. Slabko²

¹*L.V.Kirensky Institute of Physics, 660036 Krasnoyarsk, Russia*

²*Siberian Federal University, 660079 Krasnoyarsk, Russia*

(Received 11 November 2013; accepted 4 December 2013; published online 17 December 2013)

Conversion of fs supercontinuum to the ultraviolet (UV) range from 260 to 305 nm in nonlinear photonic crystal of strontium tetraborate is obtained. Spectral shape of generated UV radiation is governed by the shape of supercontinuum spectrum, focusing conditions and phase mismatch in the material of nonlinear photonic crystal. Maximum integral UV power of $2.6 \mu\text{W}$ was obtained in the case of weaker focusing, and peaks with the spectral width 1–3 nm dominate in the spectrum. Using tight focusing, broadband radiation in the range 265–300 nm was obtained.

© 2013 AIP Publishing LLC. [<http://dx.doi.org/10.1063/1.4852035>]

Obtaining supercontinuum radiation in the ultraviolet (UV) spectral region is attractive for spectroscopies and laser techniques development. When microjoule level femtosecond light sources in the near UV are used to pump homogeneous bulk media with third order nonlinearity, supercontinuum in the range 260 to 360 nm can be generated.¹ Another approach is the supercontinuum generation in gas filled photonic crystal fibers pumped by microjoule infrared fs pulses, resulting in generation within 260–300 nm range.² Second harmonic generation of visible supercontinuum in angularly phase matched crystals is of less interest due to narrow spectral bandwidth of this method, though it can be employed for supercontinuum characterization.³ Random quasi-phase-matching (RQPM) in nonlinear photonic crystals (NPC) is shown to be a method of nonlinear optical conversion with the properties that can be characterized as super-noncritical spectral and angular behavior.^{4–6} The most attractive medium for random quasi-phase-matched second harmonic of the visible and UV supercontinuum is strontium tetraborate (SBO). Transparency of this material in the vacuum ultraviolet (VUV) allows continuously tunable RQPM generation down to 121 nm.⁷ NPC SBO are as-grown ones, and their domain statistics strongly varies from one sample to another.⁸ Depending on the domain statistics, any given NPC structure can be more efficient for either UV or VUV generation. Nonlinear coefficients of SBO are among the highest for nonlinear crystals transparent below 270 nm.

In the present Letter, we report the conversion of visible fs supercontinuum to the spectral region from 260 to 305 nm. The starting laser source used was tunable Spectra Physics Tsunami Ti:sapphire fs oscillator operating at 82 MHz repetition rate. Up to 250 mW of oscillator average power was focused by $40\times$ microscope objective into 12 cm long Newport SCG-800 photonic crystal fiber (PCF) at nominal coupling efficiency 60%. Central wavelength of Ti:sapphire oscillator optimal for supercontinuum generation in our sample of PCF was typically around 780 nm. Spectral intensity of supercontinuum was dependent on the input power and at maximum of coupled power its maximum was approximately at 530 nm. Up to 100 mW of average power at the exit of PCF were collimated by $20\times$ microscope objective and then

focused into NPC SBO with another $20\times$ microscope objective. NPC sample contained 1D domain structure described in Refs. 9 and 10 with the domain walls perpendicular to a crystallographic axis (in $Pnm2_1$ space group). This structure is strongly randomized and contains domains with the thickness as large as $180 \mu\text{m}$ as well as domains with thickness below 100 nm. Distribution of domains is strongly nonhomogeneous along a axis. Input facet of NPC was parallel to the domain walls or, equivalently, normal to axis a of SBO. Supercontinuum radiation had linear polarization in the direction of c axis, and maximal nonlinear coefficient d_{ccc} of SBO was employed. Confocal parameter of supercontinuum beam cannot be directly measured in the vicinity of the second objective output. Instead of the latter, far field divergence of the supercontinuum beam after second $20\times$ objective was measured by Newport LBP-1 beam profiler. Depending on relative adjustment of two $20\times$ objectives, it could be varied from 0.4° (equivalent to confocal parameter 7 mm at 550 nm) to 11° (equivalent to $9 \mu\text{m}$ confocal parameter, half width of the spot size at $1/e^2$ level $0.9 \mu\text{m}$). Transverse distribution of supercontinuum in the far field was close to Gaussian one, with ellipticity less than 25%. Strong signal of UV was observed when confocal parameter was much smaller than the thickness of NPC structure being 2.3 mm. Radiation generated in NPC was separated from supercontinuum radiation with UV transparent filter and analyzed by Ocean Optics Maya 2000 Pro spectrometer. Spectral resolution (FWHM) of the latter was estimated with the mercury lamp to be approximately 0.3 nm. Spectral range of our Maya 2000 Pro was from 155 to 305 nm. Supercontinuum spectra were recorded via Ocean Optics HR4000 spectrometer in the range up to 1100 nm.

Fig. 1(a) presents the modification of UV spectra generated in NPC SBO during the increase of input power at the entry of PCF, accompanied by the corresponding modification of visible supercontinuum spectra (Fig. 1(b)). The range covered by UV radiation generated in NPC gradually stretches to the shorter wavelengths, and at 90 mW of spectrum-integrated supercontinuum power its most intense part lies from 265 to 295 nm. While supercontinuum spectrum in the range 530 to 590 nm is smooth, the spectrum of UV generated in NPC is of evident peaky structure. Peaks in

^{a)}Electronic mail: aleksandrovsky@kirensky.ru

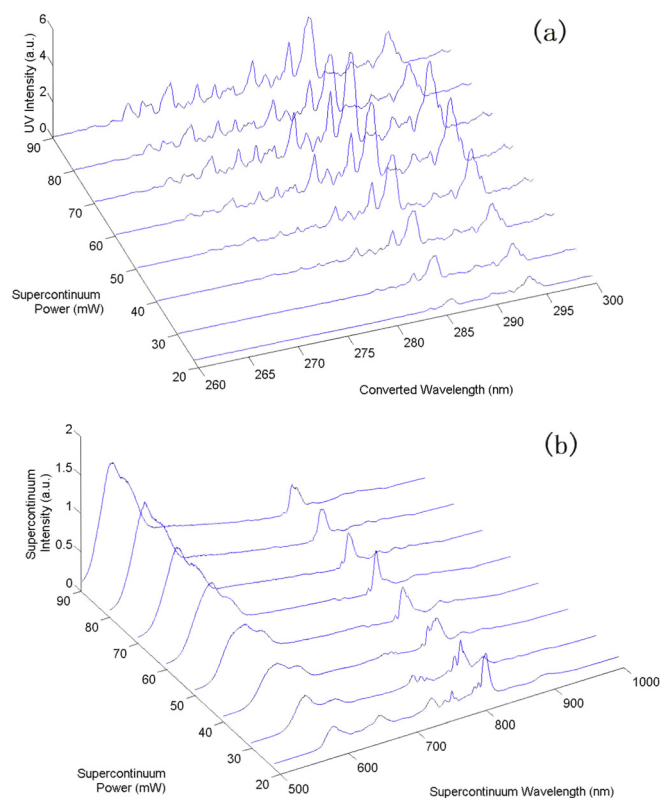


FIG. 1. (a) Spectral intensity of UV generated in NPC SBO at different spectrum-integrated powers of visible supercontinuum at the exit of PCF (b) Spectral intensity of visible supercontinuum at different spectrum-integrated powers at the exit of PCF.

the spectra of radiation generated in random NPC SBO using relatively narrowband fs fundamental radiation and relatively weak focusing were investigated in Ref. 4 and were found to be a result of interference of radiations generated in individual domains. For fixed set of domain thickness, the spectral width of peaks in conditions described above is governed exclusively by mismatch of wavevectors of fundamental and generated radiations in the material of NPC. In the plane wave approximation, typical peak width in the range of generated wavelengths below 300 nm is expected to be of order of 0.25 nm for the NPC domain structure of the sample under study. For spectra in Fig. 1(a), typical peak widths are of order of 1–3 nm and cannot be explained by instrumental broadening by spectrometer. In the present experiment, tight focusing of fundamental radiation is used, and this leads to variation of fundamental intensity in different parts of NPC. Therefore, while for plane wave nonlinear polarizations of all domains in NPC equally contribute to interference of generated radiation, for tight focusing effective number of domains contributing to interference is roughly limited to those within confocal parameter of fundamental. This circumstance must lead to broader peaks in the spectrum of generated radiation. On the other hand, examination of the spectra generated in the UV reveals the presence of broadband background, typically well seen in the range from 265 to 295 nm, with the spectral amplitude of order of 10% of peak amplitude. This background can be treated as real UV supercontinuum, and its formation is obviously due to overlapping of the wings of broadened closely spaced peaks. There is another factor that may affect spectral distribution

of generated UV, namely, summing of the non-equal frequencies within broad visible supercontinuum. This factor must have limited influence due to temporal chirp in the supercontinuum radiation emerging from PCF. For supercontinuum generator used in our experiment, this chirp can be estimated to be 9 fs/nm in the green spectral range. To compensate for this chirp, optics with opposite sign of group velocity dispersion must be used between PCF and NPC. Quoted value of chirp leads to limitation of order of 10 nm width in the spectrum of supercontinuum that can contribute to the generation at fixed UV frequency. If so, peaks with the widths noticeably larger than observed are expected in the UV. Therefore, peak widths in our case are determined by phase velocity mismatch within NPC and by focusing conditions, and compensation of supercontinuum chirp is not expected to have noticeable effect on spectra of UV radiation. Fig. 2 presents two UV spectra obtained using focused supercontinuum beams with far field divergence 3.3° and 10° , the latter spectrum being multiplied by 5. First spectrum (thin line) was obtained after adjustment of supercontinuum focusing and position of the beam within NPC in order to generate maximum UV power over the spectrum. Peaks are of order 1–2 nm wide, and continuum-like background is of order of 10% of the maximal peak. Using tighter focusing (thick line) leads to decrease of UV power, however, peaks become broader, and their overlapping forms more evident continuum-like background. Since generated power is proportional to square of both of interaction length and fundamental intensity, one must not expect drop of generated power in the case of tight focusing. Observed decrease of generated power means that in case of weaker focusing more favorable part of strongly randomized NPC structure is involved while for tighter focusing it cannot be reached via adjustment. Therefore, using NPC samples with thickness of order of 10–100 μm but with improved structure would allow obtaining broadband UV generation with enhanced power.

Frequency doubling of broadband pulses in homogeneous media may result in narrowing of the spectrum of generated radiation if spectral width of phase matching is smaller than input spectrum. For RQPM of broadband radiation, besides peaky structure discussed above, another kind of influence of phase matching conditions on generated spectra can be expected, first of all, in the case of tight focusing.

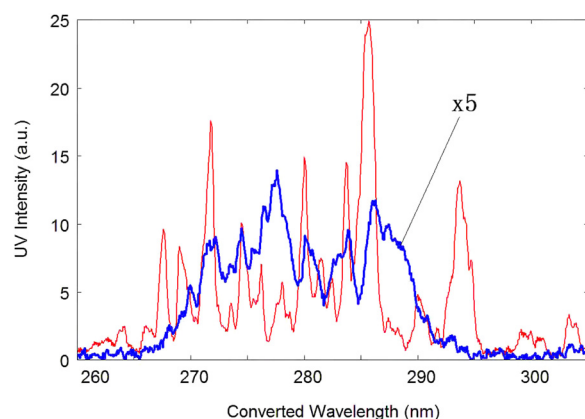


FIG. 2. Spectra of generated UV obtained in NPC SBO in case of weaker focusing (far field divergence angle $\theta = 3.3^\circ$, thin line) and tight focusing ($\theta = 10^\circ$, thick line, multiplied by 5).

Propagation of tightly focused fundamental beam through 1D NPC structure with thin enough domains may result in different phase matching conditions for different parts within the cross section of generated beam. The latter is a solution of Maxwell equations and hence, is a result of interference of fields produced by the polarization induced all over the cross section. Nevertheless, traces of the influence of the non-Gaussian generation regime may be present in the conditions of our experiment. Fig. 3 presents spectra of generated UV taken through 1 mm diameter diaphragm scanned across the beam of UV radiation. Data in Fig. 3(a) are taken with more weakly focused supercontinuum (far field divergence angle $\theta = 3.6^\circ$), and those in Fig. 3(b) are obtained with tightly focused beam ($\theta = 11^\circ$). Spectra taken at looser focusing in different parts of cross section fairly coincide in shape and relative deviation is typically less than 10%, that can be ascribed to instability of supercontinuum spectrum during measurement. Spectra taken at tight focusing in general are homogeneous across the beam, too, but relative deviations of the shape reach 35%.

Assuming that thickness of all domains in NPC is known, spectral dependence of any nonlinear optical conversion process can be calculated. Examples of these calculations are reported^{4,9} for plane wave approximation. For better agreement with the present experiment, certain

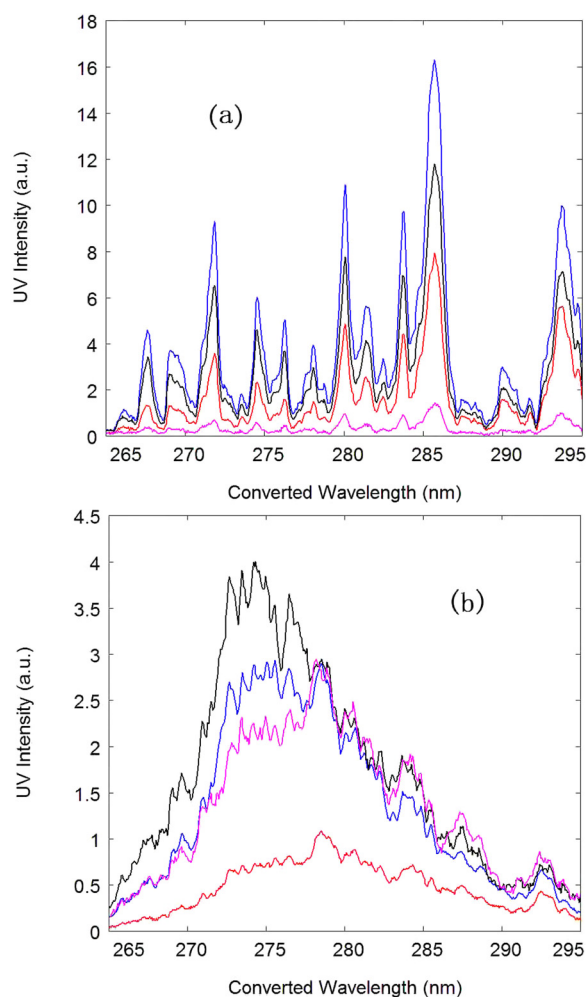


FIG. 3. Local UV spectra in different parts of the beam cross section. (a) Looser focusing ($\theta = 3.6^\circ$) (b) Tight focusing ($\theta = 11^\circ$). Distances from the beam center are, from upper to lower curve, 0, 0.5, 1, and 3 mm.

generalization of earlier approach is required. First of all, the variation of supercontinuum intensity in the vicinity of fundamental beam waist must be included. Variation of the wavefront of focused Gaussian beam can be omitted since it is expected to lead only to shift of phase matching conditions, that is, to correction of wavevector mismatch used in calculations. Second desirable modification of calculation model can be taking into account the contribution of both direct second harmonic generation and summing of non-equal frequencies within supercontinuum spectral profile to the generation at any UV wavelength. Ultimately, the field generated in an NPC structure with N domains under broadband fundamental radiation field $E_s(\lambda)$ can be approximately presented in the form

$$E(\lambda/2) = \sum_{\lambda} \sum_{j=1}^N \frac{(-1)^j}{\Delta k(\lambda_1, \lambda_2)} (\exp(i\Delta k(\lambda_1, \lambda_2)d_j) - 1) \times \exp \left[i\Delta k(\lambda_1, \lambda_2) \sum_{r=j+1}^N d_r \right] \frac{E_s(\lambda_1)E_s(\lambda_2)}{\left[1 + \left(\frac{z_j}{b/2} \right)^2 \right]},$$

where λ_1 and λ_2 are the wavelengths within supercontinuum spectrum that contribute to generation of UV radiation at the wavelength $\lambda/2$. $\Delta k(\lambda_1, \lambda_2)$ is the wave mismatch for the process of summing these photons, d_j is the thickness of j -th domain within NPC, z_j is the position of beam waist relatively to the j -th domain in NPC, and b is the confocal parameter of focusing. Sum on λ stands instead of integration over all possible pairs of λ_1 and λ_2 contributing to generation at $\lambda/2$. Phase dependence of the field $E_s(\lambda)$ on the wavelength was not included in the calculations. Example of fitting calculated spectrum to experimental one generated in NPC SBO is presented in Fig. 4. Experimental spectrum is taken at $\theta = 11^\circ$ (expected confocal parameter $b = 60 \mu\text{m}$). Calculation show that broader peaks must be present in UV spectrum at this value, and best fit is obtained at $b = 230 \mu\text{m}$. This disagreement is likely due to the fact that

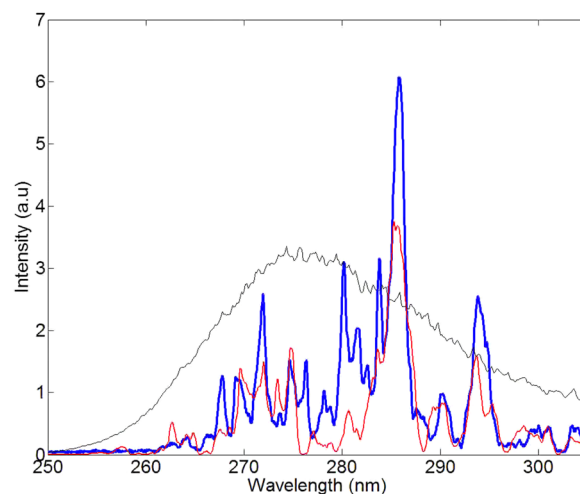


FIG. 4. Experimental (thick) and calculated (medium thick) spectra of UV generated in NPC SBO. Visible supercontinuum is shown by thin line in the wavelength scale divided by two.

supercontinuum radiation emerging from PCF is not well approximated by Gaussian beam.

Power of UV radiation was measured with the help of Newport 931C sensor in the conditions of weaker focusing and more pronounced peaky structure, since in this case UV power is larger than in the case of tight focusing. At supercontinuum power 90 mW integral UV power in the range from 250 to 305 nm was $2.6 \mu\text{W}$, efficiency being of order of 3×10^{-5} . Such efficiency level is typical for RQPM in highly randomized NPC and can be enhanced at least by the order of magnitude by using NPC with the structure optimized for the specific conversion process. Obtained result is limited by the radiation stiffness of PCF used as the source of supercontinuum, as well as the power of fs oscillator, but not by the radiation stiffness of NPC, and can be enhanced in case of more powerful supercontinuum source. Due to unique transparency of SBO, NPC based on this material are attractive for conversion of powerful UV supercontinuum sources like that described in Ref. 1 to the range 130–180 nm.

In conclusion, we obtained RQPM-enhanced nonlinear optical conversion of fs supercontinuum to the UV range from 260 to 305 nm in NPC of strontium tetraborate. Spectral shape of generated UV is governed by the shape of supercontinuum spectrum, focusing conditions and phase mismatch in the material of NPC. Maximum power of

$2.6 \mu\text{W}$ was obtained in the case of weaker focusing, and peaks with the width 1–3 nm dominate in the spectrum. Using tight focusing, broadband radiation in the range 265–300 nm was obtained.

The work was supported by the grant of President of Russian Federation MK-250.2013.2, by Projects 2.5.2 and 3.9.5 of PSB RAS.

¹P. J. M. Johnson, V. I. Prokhorenko, and R. J. Dwayne Miller, *Opt. Express* **17**, 21488 (2009).

²N. Y. Joly, J. Nold, W. Chang, P. Hölzer, A. Nazarkin, G. K. L. Wong, F. Biancalana, and P. St. J. Russell, *Phys. Rev. Lett.* **106**, 203901 (2011).

³J. M. Dudley, X. Gu, L. Xu, M. Kimmel, E. Zeek, P. O'Shea, R. Trebino, S. Coen, and R. S. Windeler, *Opt. Express* **10**, 1215 (2002).

⁴A. S. Aleksandrovsky, A. M. Vyunishev, A. I. Zaitsev, and V. V. Slabko, *Phys. Rev. A* **82**, 055806 (2010).

⁵A. S. Aleksandrovsky, A. M. Vyunishev, A. I. Zaitsev, A. A. Ikonnikov, and G. I. Pospelov, *Appl. Phys. Lett.* **98**, 061104 (2011).

⁶A. S. Aleksandrovsky, A. M. Vyunishev, A. I. Zaitsev, G. I. Pospelov, and V. V. Slabko, *Appl. Phys. Lett.* **99**, 211105 (2011).

⁷P. Trabs, F. Noack, A. S. Aleksandrovsky, A. M. Vyunishev, A. I. Zaitsev, N. V. Radionov, and V. Petrov, in *Proceedings of the 9th International Conference "UFO 2013" – Davos. 4-8 March 2013*, p. 34, Fr2.4.

⁸A. S. Aleksandrovsky, A. M. Vyunishev, and A. I. Zaitsev, *Crystals* **2**, 1393 (2012).

⁹A. S. Aleksandrovsky, A. M. Vyunishev, I. E. Shakhura, A. I. Zaitsev, and A. V. Zamkov, *Phys. Rev. A* **78**, 031802(R) (2008).

¹⁰A. M. Vyunishev, A. S. Aleksandrovsky, A. I. Zaitsev, A. M. Zhyzhaev, A. V. Shabanov, and V. Petrov, *Opt. Lett.* **38**, 2691 (2013).